Journal of Vacuum Science & Technology A

Growth of InN on Si (111) by atmospheric-pressure metal-organic chemical vapor deposition using In N Al N double-buffer layers

Zhen-Yu Li, Shan-Ming Lan, Wu-Yih Uen, Ying-Ru Chen, Meng-Chu Chen, Yu-Hsiang Huang, Chien-Te Ku, Sen-Mao Liao, Tsun-Neng Yang, Shing-Chung Wang, and Gou-Chung Chi

Citation: Journal of Vacuum Science & Technology A **26**, 587 (2008); doi: 10.1116/1.2929849
View online: http://dx.doi.org/10.1116/1.2929849
View Table of Contents: http://scitation.aip.org/content/avs/journal/jvsta/26/4?ver=pdfcov
Published by the AVS: Science & Technology of Materials, Interfaces, and Processing

Articles you may be interested in

Epitaxially grown n - Zn O Mg O Ti N n + - Si (111) heterostructured light-emitting diode
Appl. Phys. Lett. **92**, 111113 (2008); 10.1063/1.2896611

Interface reactions and Kirkendall voids in metal organic vapor-phase epitaxy grown Cu (In , Ga) Se 2 thin films on GaAs
J. Appl. Phys. **100**, 114915 (2006); 10.1063/1.2397282

In situ pendeoepitaxy of GaN using heteroepitaxial Al Ga N Ga N cracks
Appl. Phys. Lett. **89**, 024103 (2006); 10.1063/1.2219093

Nanostructural characterization and two-dimensional electron-gas properties in high-mobility Al Ga N Al N Ga N heterostructures grown on epitaxial AlN/sapphire templates
J. Appl. Phys. **98**, 063713 (2005); 10.1063/1.2060946

Misfit dislocation formation in the Al Ga N Ga N heterointerface
J. Appl. Phys. **96**, 7087 (2004); 10.1063/1.1812361

Re-register for Table of Content Alerts

Create a profile.

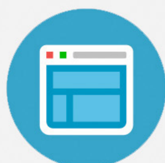

Sign up today!

Redistribution subject to AVS license or copyright; see http://scitation.aip.org/termsconditions. Download to IP: 140.113.38.11 On: Wed, 30 Apr 2014 23:01:30

Growth of InN on Si (111) by atmospheric-pressure metal-organic chemical vapor deposition using InN/AlN double-buffer layers

Zhen-Yu Li
Department of Photonics and Institute of Electro-Optical Engineering, National Chiao Tung University, 1001 Ta Hsueh Road, Hsinchu 30010, Taiwan

Shan-Ming Lan
Institute of Nuclear Energy Research, P.O. Box 3-11, Lungtan 32500, Taiwan

Wu-Yih Uen[a]
Department of Electronic Engineering, College of Electrical Engineering and Computer Science, Chung Yuan Christian University, Chung-Li 32023, Taiwan

Ying-Ru Chen, Meng-Chu Chen, Yu-Hsiang Huang, and Chien-Te Ku
Institute of Nuclear Energy Research, P.O. Box 3-11, Lungtan 32500, Taiwan

Sen-Mao Liao
Department of Electronic Engineering, College of Electrical Engineering and Computer Science, Chung Yuan University, Chung-Li 32023, Taiwan

Tsun-Neng Yang
Institute of Nuclear Energy Research, P.O. Box 3-11, Lungtan 32500, Taiwan

Shing-Chung Wang
Department of Photonics and Institute of Electro-Optical Engineering, National Chiao Tung University, 1001 Ta Hsueh Road, Hsinchu 30010, Taiwan

Gou-Chung Chi
Institute of Optical Science, National Central University, Chung-Li 32054, Taiwan

(Received 14 January 2008; accepted 21 April 2008; published 9 June 2008)

Indium nitride (InN) epilayers have been successfully grown on Si (111) substrates with low-temperature (450 °C) grown InN and high-temperature (1050 °C) grown AlN (InN/AlN) double-buffer layers by atmospheric-pressure metal-organic chemical vapor deposition (AP-MOCVD). X-ray diffraction characterizations indicated that highly (0001)-oriented hexagonal InN was grown on Si (111) substrate. Photoluminescence (PL) analyses performed at room temperature showed a strong emission at 0.72 eV with a full width at half maximum of 121 meV. Excitation intensity dependent measurements demonstrated the PL mechanism to be the band-to-band transition. Time-resolved PL could be fitted by a single exponential exhibiting an ordered film and a recombination lifetime of around 0.85 ns. In particular, transmission electron microscopy characterizations indicated that the use of AlN first buffer is very important to achieve a structurally uniform (0001)-oriented InN epilayer on Si (111) by AP-MOCVD. © *2008 American Vacuum Society.* [DOI: 10.1116/1.2929849]

I. INTRODUCTION

Indium nitride (InN) can be used in a wide range of optoelectronic applications due to its many superior properties compared to other III-V compound semiconductors. First, InN has the lowest effective electron mass, the highest electron mobility and the largest saturation velocity among all nitride semiconductors, which imply the potential applications of InN for high speed and high frequency electron devices. Alternatively, in recent years, the most striking news should be that the band gap of InN has been renewedly determined to be about 0.7–0.8 eV,[1–5] which is lower than previously reported one of approximately 1.9 eV.[6] Based on this new finding, InN can be used to combine with aluminum nitride (AlN) and gallium nitride (GaN) to produce light emitting diodes (LEDs) and laser diodes (LDs) with the luminescences covering the range from infrared to ultraviolet (0.7–6.2 eV). In addition, for the applications of solar cell, the use of InN based material system is also possible to realize an ultra-high-efficiency mutijunction tandem solar cell[7] and will replace the current high-efficiency mutijunction tandem solar cells such as InGaP/GaAs/Ge ones.[8,9] However, bulk crystal of InN is still very difficult to grow and homoepitaxial structure is not available. Only thin films of it with the monocrystallinity being emphasized were obtained by heteroepitaxial techniques, such as molecular beam epitaxy (MBE),[2,10] metal organic vapor phase epitaxy (MOVPE),[11–13] and the others.[14,15] Among the substrate materials used for epitaxial growth, Si is regarded as a relatively promising one since it has several advantages, such as low cost, large size, and high quality. Besides, the InN-on-Si ma-

[a]Author to whom correspondence should be addressed; Tel: +886-3-265-4620; electronic mail: uenwuyih@ms37.hinet.net

Redistribution subject to AVS license or copyright; see http://scitation.aip.org/termsconditions. Download to IP: 140.113.38.11 On: Wed, 30 Apr 2014 23:01:30

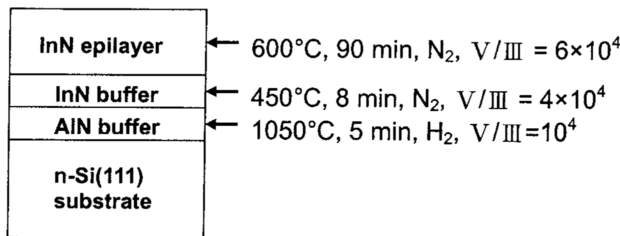

FIG. 1. Schematic of the epitaxial structure investigated.

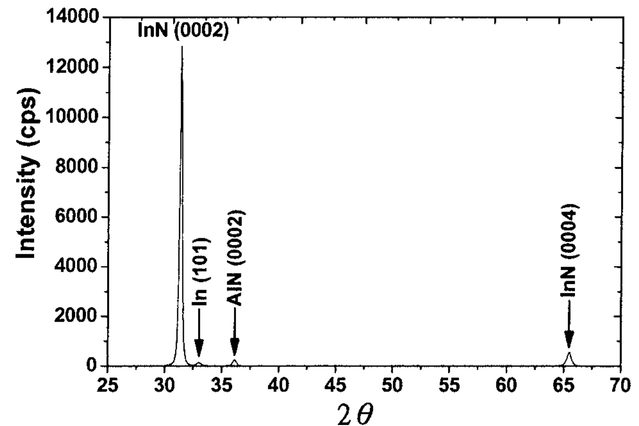

FIG. 2. Powder x-ray diffraction spectra of InN epilayers grown on Si substrate by using InN/AlN double-buffer layers.

terial system will also make possible the integration of well-developed Si-based microelectronics with III-nitride-based optoelectronics. Nevertheless, it is still difficult to grow high-quality InN on Si substrate since the InN film easily becomes polycrystalline due to the silicon nitride of amorphous phase forming on the Si substrate surface.[16] Up until now, monocrystalline InN films, which were suggested to be the requisite for presenting the luminescence band of 0.7–0.8 eV, could be successfully grown on Si mostly through MBE (Refs. 17–19) and to our best knowledge scarcely through MOVPE.[20,21] It is particularly difficult to grow InN by metal organic chemical vapor deposition (MOCVD) since the growth temperature should be kept relatively low to prevent the dissociation of InN. However, a low temperature will cause a limited cracking efficiency of NH_3, a conventional source used for nitride, and reduce the diffusivity of species arriving at the substrate surface, which influence the quality of InN grown. So far, most of the InN films grown on Si have presented photoluminescences dominated by the band around 1.6–2 eV, which is reported to be typical of polycrystalline nature.[6,22] In our previous paper, we have employed predeposited In layer and two-step growth method to grow InN epilayer on Si substrate,[23] where a GaN/AlN double-buffer structure has been grown in the first step of growth. In this work, we examine the effect of another double-buffer structure of InN/AlN on the growth of InN on Si with the characterizations of interface structure and optical properties being emphasized.

II. EXPERIMENT

InN epilayers were grown by a homemade atmospheric-pressure MOCVD (AP-MOCVD) system with a vertical reactor. The metal organic compounds of TMA, TMI, and gaseous NH_3 were employed as the reactant source materials for Al, In, and N, respectively. AlN film was grown at a molar ratio of $[NH_3]/[TMA]=10^4$ in a H_2 ambient, while InN film was grown at a molar ratio of $[NH_3]/[TMI]=4\times10^4$ in a N_2 ambient. The substrates used in this experiment were cut from (111)-oriented Si wafers with 2 in. diameter. These wafers show *n*-type conductivity with the carrier concentration around 10^{17} cm^{-3}. Prior to growth, the Si (111) substrate was etched by boiling it in $H_2SO_4:H_2O_2=3:1$ for 15 min and then dipped in HF solution ($HF:H_2O=1:10$) for 15 s to remove native oxide formed on the surface. Figure 1 shows the schematic of our epitaxial structure by using InN/AlN double buffers (denoted as sample A). First two thin films of 47-nm-thick AlN and 20-mn-thick InN were deposited in that order at 1050 and 450 °C, respectively, to form an InN/AlN double-buffer structure. Finally, the top InN layer with a thickness of approximately 250–300 nm was grown at 580 °C in a N_2 atmosphere and with the molar ratio of $[NH_3]/[TMI]=6\times10^4$. In addition, the growth of InN by using an InN single buffer (denoted as sample B) was also conducted for comparison. The crystalline quality was evaluated by powder x-ray diffraction (XRD) and Cu $K\alpha$ radiation was used as the x-ray source. The optical properties were investigated by photoluminescence (PL) measurements performed at both room temperature and 10 K, which were excited with the 488 nm line of an argon laser at excitation power densities of 6.58–8.28 W/cm^2. Besides, the recombination lifetime was determined from the time-resolved PL (TRPL) conducted at 10 K. In this case, the signal was excited by a semiconductor laser ($\lambda=976$ nm) with a pulse width of about 56 ps and a power density of 1.27 W/cm^2. For PL and TRPL measurements, the luminescence was dispersed by a 0.5 m monochromator, and was detected by an air-cooled extended InGaAs detector (with a cutoff wavelength of 2.1 μm). Furthermore, detailed structure of the InN epifilms thus grown was examined by cross-sectional transmission electron microscopy (TEM) and selected-area diffraction (SAD) analysis.

III. RESULTS AND DISCUSSION

Figure 2 shows the XRD patterns of sample A. Obviously, beside the Si (111) peak at $2\theta=28.5°$, the x-ray diffraction peaks of 31.6° and 65.6° were obtained from the (0002) and (0004) InN, respectively. A discrete diffraction spot with twofold symmetry shows highly (0001)-oriented hexagonal InN crystals were grown on the Si (111) substrate despite the weak diffraction peak at $2\theta=33.1°$, which has been assigned to the appearance of the (101) plane of metallic In by Shubina *et al.*[24] and appeared probably due to the formation of In clusters produced easily when the deposition temperature of InN is over 500 °C. No other InN phases showing polycrystalline nature of the film were observable. The XRD signal

Redistribution subject to AVS license or copyright; see http://scitation.aip.org/termsconditions. Download to IP: 140.113.38.11 On: Wed, 30 Apr 2014 23:01:30

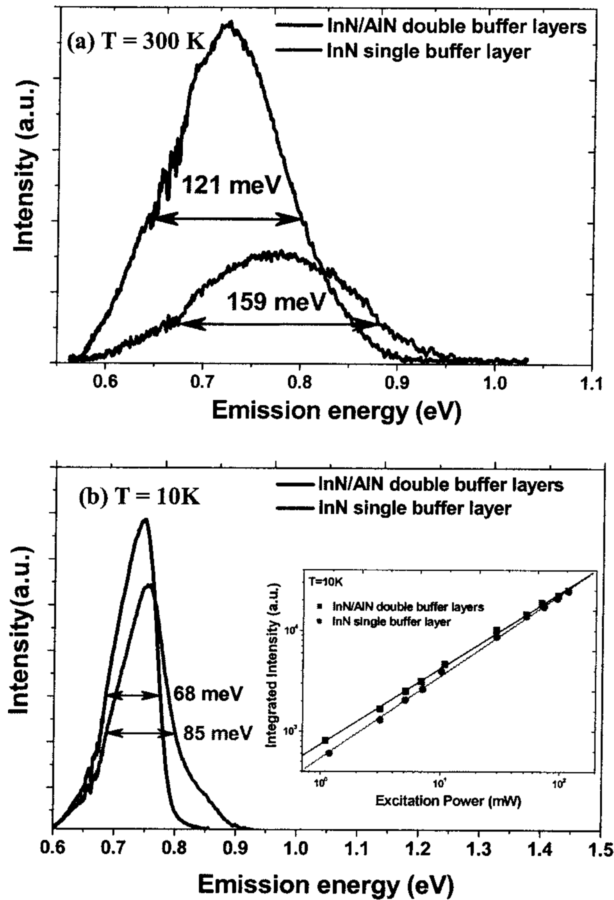

FIG. 3. (a) Room-temperature PL spectra of samples A and B. (b) 10 K PL spectra of samples A and B. The inset shows the excitation intensity dependency of the PL integrated intensity.

obtained from sample B is much the same as that of sample A except that the intensity of the (101) In peak became stronger by a factor of 2–3.

Figure 3 shows the PL spectra of samples A and B measured at (a) room temperature and (b) 10 K. The inset displays the excitation power intensity dependence of PL spectra obtained at 10 K. Regardless of the variation of measurement temperature, a very strong emission peak at 0.7–0.8 eV (1.77–1.55 μm) was observed for both samples. However, a smaller full width at half maximum (FWHM) of PL spectra was obtained from sample A, which is 121 meV at room temperature and reduces to only 68 meV at 10 K. Therefore, the optical quality of InN epilayer has been improved by using the InN/AlN double-buffer layers. Otherwise, it has been reported that the emission band of 0.7–0.8 eV probably resulted from trapping centers (originating from defects or impurities).[25] Besides, it has also been indicated that the integrated PL intensity of deep-level emissions (defects or impurities or trapping centers) increases nonlinearly with the excitation power at low excitation power levels and then tends to saturate at high excitation power levels.[6] However, as can be seen from the inset of Fig. 3(b), which exhibits the excitation power intensity dependency of integrated PL intensity for InN epilayers, the integrated PL intensity increases linearly with the excitation power intensity as reported previously[17] even after the excitation power intensity was raised to above 116 mW. It was therefore considered that the possibility of deep-level emission can be ruled out and the PL emission from our samples should be caused by a direct band-to-band emission nature and based on this the energy band gap of monocrystalline InN was resolved. Note that the shift of PL peak for both samples caused by the change in measurement temperature exhibit different tendencies. Details of this phenomenon have been systematically examined by temperature dependent PL measurements and will be reported elsewhere.

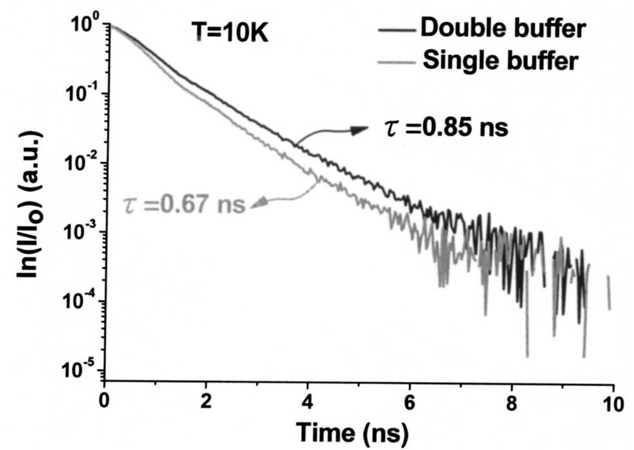

FIG. 4. 10 K TRPL measurement results for InN films with two kinds of buffer: $\ln(I/I_0)$ vs t.

Figure 4 presents the 10 K TRPL data for both samples monitored at band edge emission peak of 0.74 eV. The transients can be well fitted by the following equation:

$$I(t) = I_0 \exp\left[-\left(\frac{t}{\tau}\right)^{\beta}\right], \quad (1)$$

where $I(t)$ represents the PL intensity at time t; $I(0)\equiv I_0$, τ is the lifetime, and β the stretching parameter. The β may vary between zero and unity, providing information on the recombination mechanism. In general, the values of $\beta<1$ correspond to the existence of a broad distribution of lifetimes which describes the elementary relaxation processes whether they are radiative or nonradiative. Therefore, for $\beta\neq 1$, a stretched exponential behavior is commonly observed in PL studies of heavily disordered material systems.[26,27] From Fig. 4, one can find the recombination lifetime of about 0.85 and 0.67 ns for samples A and B, respectively. The former is longer than some previously reported value of 100 ps in Ref. 28 and therefore implies the good quality of InN epilayer by using InN/AlN double-buffer layers. Once the recombination lifetime τ is determined, the β can be extracted simply by plotting the double semilogarithm of the intensity against the semilogarithm of the time, which was found to be about 1 for both epilayers. Consequently, the TRPL spectra of the InN films grown here can be well fitted to a single exponential, which demonstrates that basically ordered films were achieved.

Redistribution subject to AVS license or copyright; see http://scitation.aip.org/termsconditions. Download to IP: 140.113.38.11 On: Wed, 30 Apr 2014 23:01:30

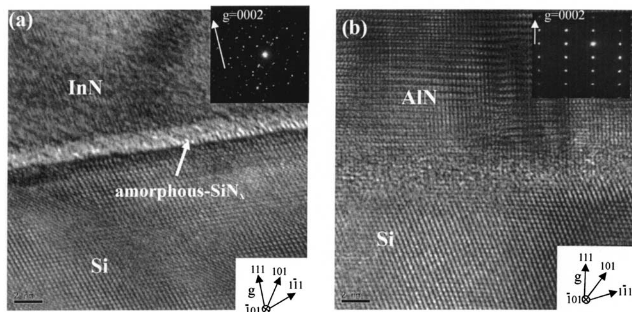

FIG. 5. High-resolution TEM cross-sectional images of InN on Si: (a) buffered by single InN layer, and (b) buffered by InN/AlN double layers. The inset shows the selected-area electron diffraction patterns of InN epilayers. The diffraction condition is g_{0002}.

Figure 5 shows the high-resolution TEM cross-sectional images of the buffer regions for the samples. Note that the inset in each figure shows the SAD pattern of top InN epilayer grown on the buffer. Obviously from Fig. 5(a), when the AlN interlayer was absent an amorphouslike SiN_x thin film was formed at the interface between InN film and Si substrate as reported in Ref. 16. In addition, a cubic structure is observed on top of that SiN_x layer, and finally the inset of Fig. 5(a) exhibits that the top InN epilayer is also of a cubic structure. Multiple SAD views on the epilayer have been taken and some of them exhibit slightly diffused spots. This might imply the top film to be composed of $\langle 111 \rangle$ oriented grains but with some metastable rotation domains. Generally, the cubic phase is associated with degradation of the crystalline quality and different directional growths undermine the quality of the film. On the other hand, Fig. 5(b) demonstrates that the formation of amorphouslike SiN_x thin film can be efficiently suppressed when the AlN buffer layer was introduced and simultaneously a wurtzite AlN layer was formed on the Si (111) substrate in spite of some interface inhomogeneities between them being in view. Further, the inset of Fig. 5(b) displays an electron diffraction pattern taken from the $\langle 10\bar{1}0 \rangle$ direction of hexagonal AlN. Clearly, a monocrystalline InN film of wurtzite structure was deposited along the c axis of AlN. This crystalline orientation has also been reflected in the XRD pattern presented in Fig. 2, wherein the (0002) peak dominates the entire spectrum. Based on the results obtained so far, the effect of InN/AlN double-buffer layers on the epitaxial growth of InN on Si (111) is considered as follows. As is known, the lattice mismatch and thermal expansion coefficient difference between InN and Si are 7.5% and 53%, respectively, while those between AlN and Si are 19% and 62%, respectively. However, the free energy of an array of strain-relaxed InN pyramids is reported to be lower than that of a continuous strained InN epilayer due to the low decomposition temperature and formation of In clusters.[29] Therefore, the InN cannot be grown as a buffer layer directly on Si substrates. On the other hand, the influence of lattice mismatch and thermal expansion coefficient incompatibility between InN and Si on the quality of InN grown is greatly suppressed once the AlN first buffer is used. AlN is reported to be a good wetting layer,[30] which can cover the Si substrate completely, prevent the formation of amorphous SiN_x thin film on top of the Si substrate, and predetermine the crystal structure of the top InN film. Hexagonal-type nucleation of InN crystallites is possible only when the first buffer of AlN is introduced. Therefore, the crystalline quality of InN epilayer can be effectively improved when an AlN buffer was deposited first, followed by a low-temperature InN buffer to nucleate homogeneously with small nuclei, which coalesce to form a continuous layer in an early stage.

As a first step to realize the effect of InN/AlN double-buffer layers on InN on Si, we have carried out the study as described above. Nevertheless, some material characteristics other than the optical properties are still left to be examined, such as the surface morphology of InN epilayer is still very rough (with a roughness of about 40–50 nm). Whether the lattice mismatch and thermal expansion coefficient incompatibility between InN and AlN rather than those between InN and Si should be responsible for this is required to be investigated further.

IV. CONCLUSIONS

InN epilayers have been successfully grown on Si (111) substrate by AP-MOCVD using InN/AlN double-buffer layers. XRD analysis indicates that the grown layer is a highly [0001] oriented wurtzite structure. Room temperature PL measurement exhibits a strong emission from InN epilayer at the energy of 0.72 eV with a FWHM of only 121 meV. Furthermore, the luminescence mechanism is considered to be the band-to-band transition based on the excitation power dependent PL characterizations. Besides, TRPL analysis exhibits that the InN epilayer buffered by InN/AlN double thin layers is a structurally uniform film with a recombination lifetime of 0.85 ns. Finally, high resolution TEM and SAD observations show that the introduction of AlN buffer suppresses the formation of amorphous SiN_x layer and enhances the growth of (0001)-oriented monocrystalline InN on Si (111).

ACKNOWLEDGMENTS

The authors are grateful to the Institute of Nuclear Energy Research (INER) for all the technical assistance. The authors would also like to thank the National Science Council of Taiwan, for financially supporting this research under Contract No. NSC 95-2221-E-033-052.

[1]V. Yu. Davydov *et al.*, Phys. Status Solidi B **229**, R1 (2002).
[2]J. Wu *et al.*, Appl. Phys. Lett. **80**, 3967 (2002).
[3]Takashi Matsuoka, Hiroshi Okamoto, Masashi Nakao, Hiroshi Harima, and Eiji Kurimoto, Appl. Phys. Lett. **81**, 1246 (2002).
[4]Y. Saito *et al.*, Phys. Status Solidi B **234**, 796 (2002).
[5]M. Hori *et al.*, Phys. Status Solidi B **234**, 750 (2002).
[6]T. L. Tansley and C. P. Foley, J. Appl. Phys. **59**, 3241 (1986).
[7]T. Yamaguchi, C. Morioka, K. Mizuo, M. Hori, T. Araki, Y. Nanishi, and A. Suzuki, 2003 International Symposium on Compound Semiconductors: Post-Conference Proceedings, 2004 (unpublished), pp. 214–219.
[8]Masafumi Yamaguchi, Takeshi Okuda, Stephen J. Taylor, Tatsuya Takamoto, Eiji Ikeda, and Hiroshi Kurita, Appl. Phys. Lett. **70**, 1566 (1997).

Redistribution subject to AVS license or copyright; see http://scitation.aip.org/termsconditions. Download to IP: 140.113.38.11 On: Wed, 30 Apr 2014 23:01:30

[9]Tatsuya Takamoto, Takaaki Agui, Eiji Ikeda, and Hiroshi Kurita, Proceedings of the 28th IEEE Photovoltaic Specialist Conference, 2000 (unpublished), pp. 976–981.
[10]J. Wu *et al.*, Appl. Phys. Lett. **84**, 2805 (2004).
[11]Qi-Xin Guo, Toshimi Yamamura, Akira Yoshida, and Nobuo Itoh, J. Appl. Phys. **75**, 4927 (1994).
[12]Akio Yamamoto, Tomohiro Shin-ya, Toshimitsu Sugiura, and Akihiro Hashimoto, J. Cryst. Growth **189/190**, 461 (1998).
[13]A. Yamamoto, Y. Yamauchi, M. Ohkubo, and A. Hashimoto, J. Cryst. Growth **174**, 641 (1997).
[14]Hai Lu *et al.*, Appl. Phys. Lett. **77**, 2548 (2000).
[15]Yuichi Sato and Susumu Sato, J. Cryst. Growth **146**, 262 (1995).
[16]Akio Yamamoto, Mitsunori Tsujino, Mitsugu Ohkubo, and Akihiro Hashimoto, J. Cryst. Growth **137**, 415 (1994).
[17]S. Gwo *et al.*, Appl. Phys. Lett. **84**, 3765 (2004).
[18]Tokuo Yodo *et al.*, J. Cryst. Growth **269**, 145 (2004).
[19]J. Grandal and M. A. Sanchez-Garcia, J. Cryst. Growth **278**, 373 (2005).
[20]A. Yamamoto, T. Kobayashi, T. Yamauchi, M. Sasase, A. Hashimoto, and Y. Ito, Phys. Status Solidi C **2**, 2281 (2005).
[21]T. Kobayashi, M. S. Chou, N. Sawazaki, A. Hashimoto, A. Yamamoto, and Y. Ito, Phys. Status Solidi A **203**, 127 (2006).
[22]Ching-Lien Hsiao *et al.*, Jpn. J. Appl. Phys., Part 2 **44**, L1076 (2005).
[23]K. J. Chang, J. Y. Chang, M. C. Chen, S. M. Lahn, C. J. Kao, Z. Y. Li, W. Y. Uen, and G. C. Chi, J. Vac. Sci. Technol. A **25**, 701 (2007).
[24]T. V. Shubina *et al.*, Phys. Rev. Lett. **92**, 117407 (2004).
[25]K. S. A. Butcher and T. L. Tansley, Superlattices Microstruct. **38**, 1 (2005).
[26]Madalina Furis, Fei Chen, Alexander N. Cartwright, Hong Wu, and William J. Schaff, MRS Symposia Proceedings Vol 743 (Materials Research Society, Pittsburgh, 2002), p. L11.14.1.
[27]Lorenzo Pavesi, J. Appl. Phys. **80**, 216 (1996).
[28]R. Intartaglia, B. Maleyre, S. Ruffenach, O. Briot, T. Taliercio, and B. Gil, Appl. Phys. Lett. **86**, 142104 (2005).
[29]L. Goldstein, F. Glas, J. Y. Marzin, M. N. Charasse, and Le Roux, Appl. Phys. Lett. **47**, 1099 (1985).
[30]Yuan Lu, Xianglin Liu, Da-Cheng Lu, Hairong Yuan, Zhen Chen, Tiwen Fan, Yufeng Li, Peide Han, Xiaohui Wang, Du Wang, and Zhanguo Wang, J. Cryst. Growth **236**, 77 (2002).

Redistribution subject to AVS license or copyright; see http://scitation.aip.org/termsconditions. Download to IP: 140.113.38.11 On: Wed, 30 Apr 2014 23:01:30